

Optical Bullet Holes: Robust Controllable Localized States of a Nonlinear Cavity

W. J. Firth and A. J. Scroggie

*Department of Physics and Applied Physics, University of Strathclyde, John Anderson Building,
107 Rottenrow, Glasgow G4 0NG, United Kingdom*

(Received 21 August 1995)

Stable localized states are predicted for a saturable absorber in an optical cavity. These “bullet holes” resemble 2D spatial solitons, and we demonstrate an optical memory array scheme based on them. A topological argument shows that one or more unstable localized states coexist with the stable bullet hole.

PACS numbers: 42.65.Sf, 42.65.Tg

Stable localized states are among the most interesting spatiotemporal structures exhibited by extended nonlinear systems. If robust, they are also interesting—especially in optics—as “bits” for parallel information storage and processing. One could envisage such structures as the two-dimensional spatial analogs of the temporal solitons which promise to revolutionize long-distance telecommunications [1]. The flaw in a straightforward analogy is that the nonlinear Schrödinger equation (NLS) has stable solitons only in (x, t) , while in (x, y, t) the “solitons” are unstable, collapsing to a singularity [2]. Localized states have also been examined in Ginzburg-Landau equations, usually concentrating on “pulses” in just one spatial dimension [3].

Here we present analytical and numerical evidence for the existence of stable two-dimensional (2D) localized states (LS) in a driven optical cavity containing a saturable absorber. In transmission these would appear as transparent disks on an absorbing background, most simply formed by aiming a short pulse of light at the target location. These two attributes prompt the term “optical bullet holes” (OBH). The long-term prospect of very fast, micron-scale, generation using “optical bullets” [4] is an additional motivation and an attractive prospect. Unlike real bullet holes, OBH can be moved around, and we demonstrate a self-correcting control scheme for the address “bullets” in 2D OBH arrays.

While our results are founded on numerical evidence, we take advantage of cylindrical symmetry to demonstrate a simple, but robust, topologically based method for locating the LS and demonstrating their stability. This approach should be widely applicable in situations where 2D LS are at issue, especially because it does not require any assumptions about near integrability of the governing equations, or smallness of amplitude of the solution.

We study the mean-field ring cavity model for a two-level medium [5,6]. In the good cavity limit, with fast relaxation of the medium variables, the system may be described by a single partial differential equation in the complex field E ,

$$\partial_t E = -E \left[(1 + i\theta) + \frac{2C(1 - i\Delta)}{|E|^2 + 1 + \Delta^2} \right] + E_I + ia\nabla^2 E. \quad (1)$$

Here θ is the cavity mistuning parameter, E_I is the external pump field, Δ is the detuning of its frequency from the medium resonance, and $2C$ is the medium density expressed as an optical absorptivity. The time has been scaled to the decay rate of the intracavity field, and the fields to the square root of saturation intensity. The diffraction parameter $a = L_{\text{eff}}/k$, where k is the optical wave vector and L_{eff} is the effective cavity length [5].

The purely absorptive ($\Delta = 0$) case has the advantage of algebraic simplicity, and offers an example of structure formation with absorptive nonlinearity [6]. We assume this case below, except where Δ appears explicitly. Then time-independent, spatially homogeneous solutions E_s of Eq. (1) obey

$$\frac{E_I}{E_s} = 1 + i\theta + \frac{2C}{1 + |E_s|^2}, \quad (2)$$

and, depending on the values of θ and C , the plane-wave input-output characteristic may be either monostable or bistable. Previously, LS in this system have been predicted for the bistable case, where they were termed “diffractive autosolitons” and viewed as mutually trapped switching waves linking the two stable states [7], and, independently, for the special case of “nascent bistability” [8]. Here we deal with stable OBH in the monostable regime, demonstrating that they are a phenomenon independent of bistability.

E_s has a modulational instability (MI) for $IS > S + 1$, where $I = |E_s|^2$ and $S = 2C/(I + 1)^2$ is a saturation parameter, as was first shown in [5]. We will be concerned with the region below this MI threshold where a solitary wave structure can sit on a *stable* homogeneous background.

The unstable wave vector at MI threshold has magnitude $K_c = \sqrt{-\theta/a}$, which is real only if θ is negative. The generated off-axis field then propagates at an angle which exactly compensates the cavity mistuning [6]. We interpret the OBH in a similar vein: At its center the OBH profile allows the Laplacian term in (1) to cancel the mistuning term, enabling resonant excitation and consequent bleaching. The OBH acts a self-induced waveguide, with the guidance provided by the (negative) loss profile—for $\Delta = 0$ there is no linear or nonlinear index profile.

We begin with results on creation and control of OBH in a full numerical simulation. We integrate the partial differential equation (1) on a square grid using a split-step method. The OBH are created by an initial Gaussian pulse of amplitude greater than, and width comparable to, the solution sought. One can also track an OBH branch across some parameter range.

The inset in Fig. 1 shows a typical OBH. Relative to the background field E_s , it has a strong central peak surrounded by a fairly shallow trough. Figure 1 itself shows the OBH plotted in the complex E plane and for comparison the E values of the coexisting hexagonal pattern. The similarity invites interpretation of these hexagons as a close-packed lattice of OBH. Also shown is a cylindrically symmetric OBH solution $E(r)$ computed directly from Eq. (1)—see below. The excellent match lends confidence in these results.

The number and location of OBH depends only on the system's history (address pulses), and not on the steady input field, so they can be used as bits in an optical memory. If N OBH can exist without undue interaction in the available transverse area, one can divide it into N pixels, each of which can contain just one or zero OBH. This gives 2^N coexistent stable states, i.e., an N -bit memory.

Pixel functions with some kind of "potential well" attract OBH more effectively to its center and inhibit noise-induced drift. To this end, note the invariance of (1) under a constant phase shift of both E and E_I . This

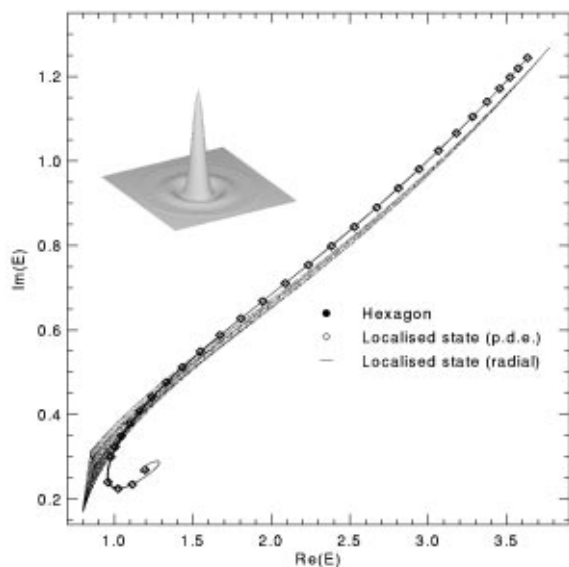


FIG. 1. Plot in the complex E plane of the stable localized state obtained from both two-dimensional simulations (diamonds) and radial integration (solid line) for $\theta = -1.2$, $C = 5.4$, and $I = 1.5$. Also plotted is the coexistent stable hexagonal solution. The localized state solutions spiral out from, and eventually back into, the plane-wave fixed point (bottom left). The inset in the top left shows $|E|$ plotted in the transverse plane for the stable OBH.

global gauge invariance can be extended to the case of tilted wave fronts: $E_I = E_{I_0} e^{i\mathbf{K}\cdot\mathbf{x}}$, $E = F e^{i\mathbf{K}\cdot\mathbf{x}}$, where \mathbf{K} is a constant vector. From Eq. (1), F must obey

$$[\partial_t + (2a\mathbf{K} \cdot \nabla)]F = -F - i[\theta + aK^2]F + E_{I_0} - \frac{2C(1 - i\Delta)F}{1 + \Delta^2 + |F|^2} + ai\nabla^2 F. \quad (3)$$

The time derivative has become a convective derivative, and so any static solution which exists for an aligned input ($\mathbf{K} = 0$) should survive but move with velocity $2a\mathbf{K}$ on misalignment. That misalignment leads to a lateral drift of optical patterns has been found in several systems [9,10], but its connection to phase symmetry, and thus its generality, has not been stressed (though mentioned in [11] in a laser model).

Consider now a more general space-dependent phase modulation:

$$E_I = E_{I_0} e^{i\phi(x,y)}, \quad E = F e^{i\phi(x,y)}. \quad (4)$$

Under this local gauge transformation the damping and detuning coefficients develop a spatial dependence, and the drift velocity of the solution is now given by $\mathbf{v} = 2a(\nabla\phi)$. In consequence, an OBH will move towards the local maximum of $\phi(x,y)$ and remain there, and so a pixel array can be made if ϕ has an array of maxima. In Fig. 2 we write the letters "IT" in such a four-by-four pixel array. Large errors in address location were imposed to demonstrate that here the address tolerance is the pixel pitch, typically several times larger than the island size limiting the address tolerance of material pixels [12].

Figure 1 suggests that LS are stationary, localized, cylindrically symmetric solutions of Eq. (1). We now obtain and discuss such solutions, which we write in the form $E(r) = E_s[1 + A(r)]$, where evidently $A(r)$ must vanish at large r for LS. At the origin, appropriate boundary conditions are $A(0) \equiv A_0 \neq 0$ and $\partial_r A(0) \equiv A_r(0) = 0$. More general "ring" LS with $A(0) = 0$ may exist, but are not considered here.

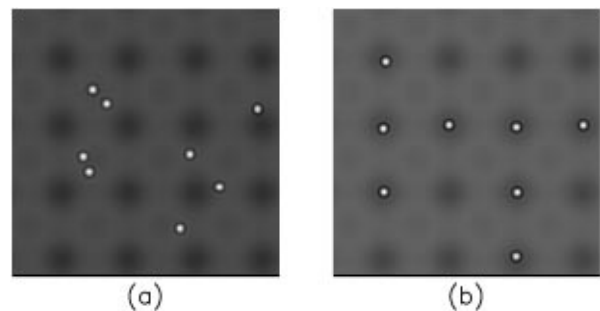


FIG. 2. Writing the letters IT in localized states on a square array of pixels created by a phase modulated pump. The real part of the field E is shown at (a) $t = 20$ and (b) $t = 800$ cavity lifetimes. $\theta = -1.2$, $E_I = 6.65$, and $C = 5.4$.

An instructive approach to finding LS is to integrate Eq. (1) inward towards $r = 0$, starting at a large radius r_1 where it can be linearized, and thus $A(r)$ obeys

$$a\nabla^2 \begin{bmatrix} A \\ A^* \end{bmatrix} = \begin{bmatrix} \theta - i(S+1) & iIS \\ -iIS & \theta + i(S+1) \end{bmatrix} \begin{bmatrix} A \\ A^* \end{bmatrix} = \mathcal{M} \begin{bmatrix} A \\ A^* \end{bmatrix}. \quad (5)$$

The eigenvalues of \mathcal{M} are obviously relevant: They are

$$\Lambda_{\pm} = \theta \pm i[(S+1)^2 - I^2 S^2]^{1/2}. \quad (6)$$

Because $S+1 > IS$ in the LS regime (below the MI threshold), we can define

$$\lambda = \left(\frac{\Lambda_+}{a}\right)^{1/2}, \quad \text{Re}\lambda > 0. \quad (7)$$

Then a general solution of (6) which decays as $r \rightarrow \infty$ is

$$A_{\infty}(r) = BK_0(\lambda r)e^{-\varphi} + [BK_0(\lambda r)]^* e^{\varphi}. \quad (8)$$

K_0 is a generalized Bessel function and $\varphi > 0$ obeys $S+1 = IS \cosh(2\varphi)$. B is an arbitrary complex constant, the choice of which uniquely parametrizes *localized* solutions to the *nonlinear* equation (1). Our task is to find values of B which generate solutions obeying the LS boundary condition at $r = 0$.

To accomplish this, we fix r_1 appropriately (typically $r_1 \sim 20\sqrt{a}$), choose B , initialize $A(r_1)$ and $A_r(r_1)$ using (8), and integrate (1) inward to $r = r_0 \sim 0$. Define $f(B) = \lim_{r_0 \rightarrow 0} A_r(r_0)$. For most B , f diverges logarithmically, but there will be curves of initial conditions in the complex B plane for which $\text{Re}f = 0$, and others for which $\text{Im}f = 0$. Apart from the special case $B = 0$ (which generates the flat solution $A \equiv 0$), *intersections of these curves define LS*. For this case, and for many other nonlinear spatiotemporal systems, these curves are continuous and reasonably well behaved. Their intersections are therefore topological features, robust against small changes in parameters (such as I , C , Δ , and θ in the present case). For the same reason, the existence and properties of LS found by this approach are not sensitive to the type and accuracy of the numerical methods used to find them.

Figure 3 shows $|A_0|$ for the LS solutions as a function of I for the monostable case $C = 5.4$, $\theta = -1.2$. For comparison, the corresponding A_0 values obtained from the simulations are shown, and there is clearly excellent agreement.

Note that a *pair* of solutions appears at $I \approx 1.1$ in what appears to be a saddle-node bifurcation. It follows from our association with curve crossings in the B plane that LS are always created and destroyed in pairs, forming multiple branches coexistent with the flat background. Figure 3 also shows a third branch, which at I around 1.54 collides with the OBH branch observed in the simulations, precisely where that OBH seems to lose stability.

We have been able to infer the linear stability of all these solutions by a method somewhat similar to our

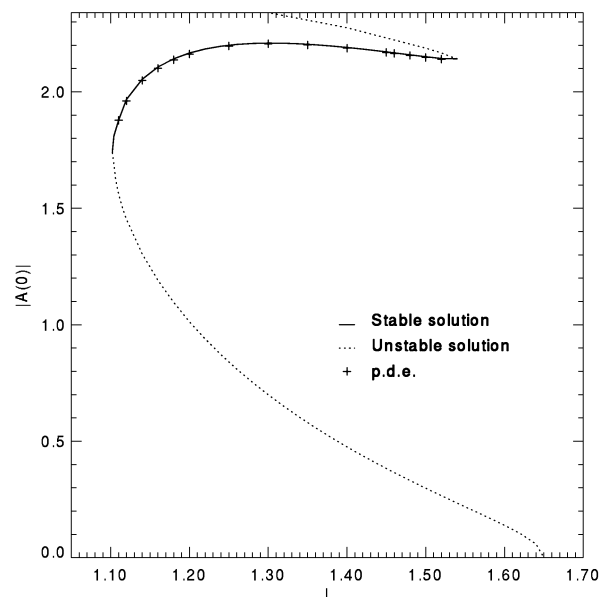


FIG. 3. Bifurcation diagram showing $|A(r=0)|$ for the stable OBH branch and the two unstable solution branches with which it collides, as a function of I ($\theta = -1.2$, $C = 5.4$). The values were calculated by radial integration of the time-independent system. Also shown are the results from two-dimensional simulations indicating excellent agreement.

radial-integration search technique for finding the solutions themselves. The search in this case is over the complex growth rate β of the perturbation. For all LS discussed, the largest growth rate is *real* and follows the pattern implied by Fig. 3, with only the middle branch being stable. At $I = 1.5$, the growth rates are $\beta = +0.14, -0.11, +0.90$ for the lowest, middle, and uppermost branches in Fig. 3, consistent with simulations. Although we have dealt here only with cylindrically symmetric states, the search method, and more importantly the stability analysis, is readily extended to include states and perturbations with an azimuthal variation.

From our analysis it follows that at any value of I the number of LS must be *even*, so the three branches in Fig. 3 imply a fourth. We plot all four LS for $I = 1.5$ in Fig. 4. The two states about to merge and annihilate around $I = 1.54$ are already quite similar, but the “fourth” is quite different, with a weak central peak and a much stronger ring than the others. Are these four the entire set? No. In fact, for $I = 1.5$ there are at least *ten*. We note that multiple LS have been found previously for the 2D NLS [13].

None of the previous investigations of 2D LS in optical cavities have gone beyond simulation. This work identifies the existence of multiple branches for the first time, and shows the bifurcation scenario underlying the numerical observations of OBH. Our methods for the identification and tracking of such states provide a powerful search method for LS in other systems, whether optical or not.

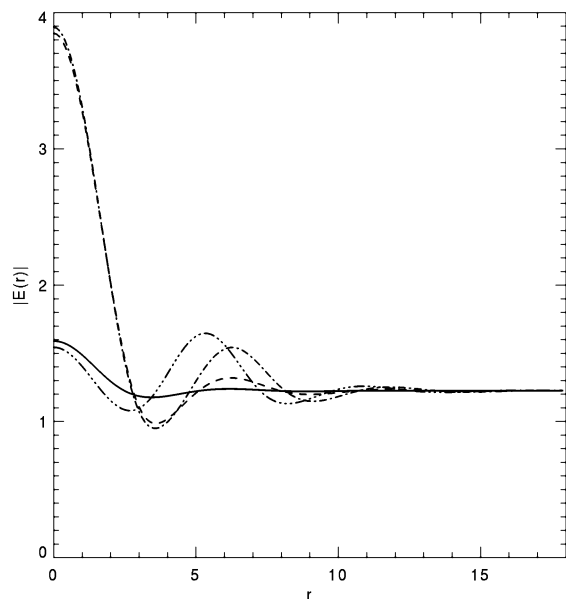


FIG. 4. Plot of $|E|$ as a function of r for four OBH found as solutions of the time-independent system with $\theta = -1.2$, $I = 1.5$, and $C = 5.4$.

Admittedly, the “new” branches discovered here are unstable, but unstable states are important for understanding and interpreting system behavior. For example, the unstable lowest branch will determine the switching threshold for the OBH memory array described earlier. Further, this branch collides with the background solution precisely at the MI threshold. This is a general feature, which enables any stable branches to be found by continuous tracking of the unstable branches, starting from the known MI threshold.

In this paper we predict the existence of stable, controllable optical bullet holes for a saturable absorber in an optical cavity. These possess at least some of the desirable features of 2D spatial solitons, and we have demonstrated a simple but instructive method by which they can be manipulated and controlled to form a 2D optical memory array. We have shown that these states have topological aspects which make them physically and numerically robust, and therefore should be experimentally demonstrable. An interesting possibility lies in semiconductor microstructures. Semiconductor lasers are describable by a model which is essentially (1), with the linewidth enhancement factor playing the role of Δ , and some extra features to describe spontaneous emission, carrier dynamics and dif-

fusion, and so on [14]. Optical bistability, which is readily observable in these systems, requires parameters similar to those leading to OBH formation.

Semiconductor microstructures lend themselves to miniaturization, prompting the question of how small these OBH can be made. Although the present model (1) relies on the paraxial approximation, recent work on microfeedback structures [15] shows that nonparaxial localized states exist in a model closely similar to the present one. With the right materials, and bulletlike address pulses, there are prospects of wavelength-scale parallel information storage and processing based on these OBH.

We are grateful to M. Brambilla, L. A. Lugiato, and B. Samson for access to results prior to publication, and to A. Lord for some numerical results. This work was supported in part by ESPRIT Grant No. 7118 (TONICS), and in part by EPSRC Grant No. GR/J 30998. A. J. S. acknowledges an EPSRC studentship.

-
- [1] *Optical Solitons—Theory and Experiment*, edited by J. R. Taylor (Cambridge University Press, Cambridge, 1992).
 - [2] J. J. Rasmussen and K. Rypdal, *Phys. Scr.* **33**, 481 (1986).
 - [3] M. C. Cross and P. C. Hohenberg, *Rev. Mod. Phys.* **65**, 851 (1993).
 - [4] Y. Silberberg, *Opt. Lett.* **15**, 1282 (1990).
 - [5] L. A. Lugiato and C. Oldano, *Phys. Rev. A* **37**, 3896 (1988).
 - [6] W. J. Firth and A. J. Scroggie, *Europhys. Lett.* **26**, 521 (1994).
 - [7] N. N. Rosanov, *J. Opt. Soc. Am. B* **7**, 1057 (1990).
 - [8] M. Tlidi, P. Mandel, and R. Lefever, *Phys. Rev. Lett.* **73**, 640 (1994).
 - [9] M. Haelterman and G. Vitrant, *J. Opt. Soc. Am. B* **9**, 1563 (1992).
 - [10] G. Grynberg, *Opt. Commun.* **109**, 483 (1994).
 - [11] N. N. Rozanov, A. V. Fedorov, S. V. Fedorov, and G. V. Khodova, *JETP* **107**, 376 (1995).
 - [12] J. L. Oudar, B. Spez, R. Kuszelewicz, J. C. Michel, and R. Azoulay, *Phys. Status Solidi B* **159**, 181 (1990).
 - [13] H. A. Haus, *Appl. Phys. Lett.* **8**, 128 (1966); Paul K. Newton and Shinya Watanabe, *Physica (Amsterdam)* **67D**, 19 (1993).
 - [14] A. Hohl, H. J. C. van der Linden, R. Roy, G. Goldsztein, F. Broner, and S. H. Strogatz, *Phys. Rev. Lett.* **74**, 2220 (1995).
 - [15] W. J. Firth, Yu. A. Logvin, and B. A. Samson, *NDOS'95*, TA5, Rochester (1995).